HHS Public Access

Author manuscript

Neuroimage. Author manuscript; available in PMC 2021 January 15.

Published in final edited form as:

Neuroimage. 2020 January 15; 205: 116237. doi:10.1016/j.neuroimage.2019.116237.

Mapping critical cortical hubs and white matter pathways by direct electrical stimulation: an original functional atlas of the human brain.

Silvio Sarubbo, MD, PhD[1,*,^], **Matthew Tate, MD, PhD**[2,*], **Alessandro De Benedictis, MD, PhD**[3], **Stefano Merler, PhD**[4], **Sylvie Moritz-Gasser, PhD**[5,6], **Guillaume Herbet, PhD**[5,6], **Hugues Duffau, MD, PhD**[5,6]

[1]Division of Neurosurgery, Structural and Functional Connectivity Lab Project, Azienda Provinciale per i Servizi Sanitari (APSS), 9 Largo Medaglie d'Oro, 38122 Trento (Italy)

[2]Departments of Neurosurgery and Neurology, Northwestern University, Feinberg School of Medicine, 420 E Superior St, 60611 Chicago, IL (USA)

[3]Neurosurgery Unit, Department of Neuroscience and Neurorehabilitation, Bambino Gesù Children's Hospital IRCCS, 4 Piazza Sant'Onofrio, 00165 Rome (Italy)

[4]Bruno Kessler Foundation (FBK), Trento (Italy)

[5]Department of Neurosurgery, Gui de Chauliac Hospital, Montpellier University Medical Center, 80 Avenue Augustin Fliche, Montpellier (France)

[6]National Institute for Health and Medical Research (INSERM), U1051, Team "Plasticity of the Central Nervous System, Human Stem Cells and Glial Tumors", Institute for Neurosciences of Montpellier, Montpellier University Medical Center, 80 Av Augustin Fliche, Montpellier (France)

Abstract

Objective: The structural and functional organization of brain networks sub-serving basic daily activities (i.e. language, visuo-spatial cognition, movement, semantics, etc.) are not completely understood to date. Here, we report the first probabilistic cortical and subcortical atlas of critical structures mediating human brain functions based on direct electrical stimulation (DES), a well-validated tool for the exploration of cerebral processing and for performing safe surgical interventions in eloquent areas.

^**Corresponding Author***Silvio Sarubbo*, MD, PhD, Division of Neurosurgery, Structural and Functional Connectivity Lab Project, "S. Chiara" Hospital, Azienda Provinciale per i Servizi Sanitari (APSS), 9, Largo Medaglie d'Oro, 38122 Trento, Italy, silviosarubbo@gmail.com.

*These authors contributed equally.

Disclosures: No authors have disclosures or conflict of interest regarding this work.

Ethics Statement

The present study has been carried out in accordance with The Code of Ethics of the World Medical Association (Declaration of Helsinki) for experiments involving humans and was approved by the local Institutional Review Board.

Methods: We collected 1162 cortical and 659 subcortical DES responses during testing of 16 functional domains in 256 patients undergoing awake surgery. Spatial coordinates for each functional response were calculated, and probability distributions for the entire patient cohort were mapped onto a standardized three-dimensional brain template using a multinomial statistical analysis. In addition, matching analyses were performed against prior established anatomy-based cortical and white matter (WM) atlases.

Results: The probabilistic maps for each functional domain were provided. The topographical analysis demonstrated a wide spatial distribution of cortical functional responses, while subcortical responses were more restricted, localizing localized to known WM pathways. These DES-derived data showed reliable matching with existing cortical and WM atlases well as recent neuroimaging and neurophysiological data.

Conclusions: We present the first integrated and comprehensive cortical-subcortical atlas of structures essential for humans' neural functions based on a highly-specific DES mapping during real-time neuropsychological testing. This novel atlas can serve as a complementary tool for neuroscientists, along with data obtained from other modalities, to improve and refine our understanding about the functional anatomy of critical brain networks.

Keywords

Atlas; Brain Functions; Brain Mapping; Direct Electrical Stimulation; White Matter

INTRODUCTION

Since the origin of the medical sciences, the brain has been considered the most complex human organ and the core of human intelligence.[1,2] Over the last three decades, the exploration of brain structures and functional processing experienced substantial advances, most notably due to non-invasive neuroimaging techniques such as functional MRI (fMRI) and diffusion-weighted imaging (DWI) tractography. Task-based and resting-state fMRI provided insights into the functional organization and plasticity of brain networks, while DWI offered visualization of white matter (WM) pathways underlying network connectivity, opening the era of the brain connectome.[3] The integration of fMRI, lesion maps,[4] and tractography provided notable contributions to the definition network circuitry underlying brain processing[5] and a large volume of original data. Despite their obvious importance in neuroscience research, fMRI and DTI do have some limitations.[6-8] For instance, while fMRI may delineate which brain areas involved in a given function, it does not indicate which of these regions are critical, and DTI, despite its interest and widespread adoption into neuroscience over the last decade, does not provide functional information about human WM pathways. Thus, there is a critical need for simple, direct, and reproducible measurements of brain function that can serve as a starting point for a more sophisticated understanding of human brain network organization and function.

In this context, the application of cortical-subcortical direct electrical stimulation (DES) during resection of low-grade gliomas (LGGs), allowed reliable, original and reproducible evidence for the functional assessment of different brain networks.[9-13] Moreover, despite the fact that LGGs infiltrate cortical and subcortical WM sites, this method has demonstrated

added contributions relative to other brain mapping techniques [i.e. electro-encephalography, cortico-cortical evoked-potentials, transcranial magnetic stimulation (EEG, CCEPs, TMS)].[14-16] In particular, DES is currently considered the primary technique in neurosurgical practice for the identification of critical network components at both the cortical and the subcortical levels, allowing neurosurgeons to preserve neurologic functions despite resections in or near eloquent areas.[17-19] It is worth noting that DES is not the only technique that provides information about the putative properties of the cortices, but it does constitutes the unique method to investigate the functional role also of WM connections during mapping. Thus DES has allowed the computation of cortical and subcortical, probabilistic functional atlases of the human brain that are consistent with the current neuroscience literature.[20-23] However, no studies are available integrating cortical and subcortical DES data for a given function, nor validating such findings using independent non-DES data sets.

Here, we propose, for the first time to our knowledge, an integrated probabilistic atlas of the critical hubs and connections subserving fundamental human brain functions, based on a series of 1821 functional responses collected by DES in 256 patients undergoing awake craniotomy. We defined these maps according to a comprehensive and practical description of the cortical and subcortical brain regions required for key domains of human brain processing, as determined by DES during real-time neuropsychological evaluation. For each individual functional response evoked during DES, we provide MNI coordinates, with the goal of proposing a practical and complementary atlas for supporting, refining, validating, and driving brain network analyses.

MATERIAL AND METHODS

Patient characteristics and intraoperative mapping paradigm

256 patients [mean age: 38.7 years] with WHO grade II LGGs were included (demographics and general information are reported in Table 1). An asleep-awake-asleep protocol was utilized, with sedation stopped just prior to the awake mapping portion of the surgery.[21,22,24] DES was performed to identify essential cortical epicenters and subcortical pathways, according to the technique previously reported.[13,19,21,22,25,26] Briefly, a bipolar electrode with 5 mm spacing was used to deliver a biphasic current to the brain surface or subcortical white matter (60 Hz; 2-4 mA; 1 msec pulse duration). During awake mapping, the DES intensity threshold was determined by either evoking speech arrest (without facial or tongue movements) during a counting task (from 0 to 10) within the ventral pre-motor cortex (VPMC) or by evoking motor (i.e. muscle contraction) and/or sensory (i.e. dysesthesias) responses during stimulation of the primary motor or sensory areas [the pre-central (Pre-CG) or post-central gyrus (Post-CG), respectively]. This threshold was used for the remainder of the mapping session. The entire exposed cortical surface was electrically interrogated, even beyond the borders of the lesion, to define a map of functionally critical brain regions (Figure 1). During the tumor resection, patients were asked to continuously perform specific tasks that were designed according to the cortical and subcortical pathways that the neurosurgeon was expected to encounter during resection (rather than all 16 tasks at each cortical/subcortical site, which would have been impractical given intraoperative time

limitations). For the purposes of this study, subcortical mapping referred to the WM bundles and/or caudate/basal ganglia that was exposed at the depth of the surgical resection cavity. The entire area of subcortical WM exposed during the resection was mapped using the same current threshold identified during the initial cortical mapping (Figure 1). With respect to DES-defined mapping sties, a “positive” functional site referred to a cortical/subcortical region that either promoted a functional response (in the case of motor and sensory mapping) or altered normal behavior (in the case of all other functional categories tested). Specific examples of positive functional mapping sites are detailed below in the “Neuropsychological Testing” section.

When all functional limits of the resection were reached (i.e. the boundaries of the surgical cavities resulted in eloquent responses with DES at both the cortical and subcortical levels), the resection was stopped. Functional responses were marked with numerical tags, and intra-operative digital images of the cortical and subcortical DES-defined maps were stored for offline analyses, specifically direct comparison with the pre- and post-operative anatomic MRI.

Neuropsychological testing

Motor functions were monitored in two ways: (1) overt muscle twitch noted during cortical or subcortical stimulation and (2) alteration of a continuous complex motor task (simultaneous hand, arm and forearm flexion-extension contralateral to the lesion side) during stimulation, specifically acceleration, deceleration, halting of movement. Sensory responses were reported verbally by the patient during cortical and subcortical mapping, in particularly dysesthesias of the contralateral face, arm, or leg during stimulation.[27,28] Spontaneous language production was monitored by a counting paradigm (series from 0 to 10) and repetition test, with positive functional responses being involuntary cessation of counting or inability to repeat, respectively, during stimulation.[29,30] Phonologic and semantic aspects of language processing (i.e. semantic and phonological paraphasias or pure anomia, not related to motor/praxis/visual disturbances) and reading (i.e. alexia or reading disturbances) were assessed with picture naming [denomination object 80 (DO 80)] and reading tests, respectively, as previously reported.[27,28,30-32] Examples of positive functional responses included semantic paraphasias (e.g. patient says “dog” instead of cat during presentation of a picture of a cat), phonemic paraphasias (e.g. patient says “kite” instead of cat after presentation of a picture of a cat), and anomias (e.g. patient states “this is a .....” but cannot come up with “cat” during presentation of a cat picture). Such patient errors during stimulation were monitored by a speech therapist (S.M-G.) or by a neuropsychologist (G.H.). Non-verbal semantic disorders (namely, asemantism) were identified with the pyramid-palm-tree test (PPTT). For the PPTT, a picture is shown and the patient asked to select the one picture (from a choice of two) that goes with the original picture.[33,34] Visual field, visual functions and eye movements were monitored, as previously described.[35-37] Spatial cognition was assessed with a line bisection task, according to the technique previously described, where the patient is presented with a standard length line and asked to mark the midpoint with a pen.[10,38] Functional responses related to mentalizing (i.e. understanding, and consequently predicting, mental and psychological states and behaviors) were assessed using a variant of the classical Reading the Mind in the Eyes Test,[34] in which

the patient is presented with a set of eyes and then asked to choose (from a list of four) the emotional state. Importantly, during these tasks, both the patient and neuropsychologist/ speech therapist were blinded to the timing of DES performed by the surgeon.

Atlas computation

All patients underwent volumetric T1-weighted MRI with gadolinium 3 months after surgery. These sequences were normalized spatially to the Montreal Neurologic Institute (MNI) 152 template brain space, at $1mm^3$ voxel spatial resolution.[39] Non-brain structures were removed from the T1-images with the brain extraction tool (BET) of the FMRIB software library (FSL; http://www.fmrib.ox.ac.uk/fsl). Registration of resulting images was performed by applying 12 parameter affine transformations using FSL's linear image registration tool (FLIRT). Of note, this method proved more reliable than non-linear registration methods that were explored due to factors specific to patients harboring brain tumors (brain shift, local mass effect, sizeable resection cavity, ventricular changes). As previously described,[13,21,22,24] the MNI coordinates of the functional subcortical and cortical responses, collected during intra-operative DES, were extracted by the first and second authors (S.S. and M.T.), two expert anatomists with previous experiences in these atlas methods. Each stimulation point was manually plotted onto a digitized asymmetric human brain template (MNI ICBM152, 1-mm resolution) using a combination of regional cortical (sulci, vessels) and subcortical (resection cavity) landmarks, T1-weighted MRI reconstructed on three planes (axial, sagittal and coronal), and dictated operative reports. Three-dimensional coordinates (x, y, z) in MNI space were recorded and reported for each cortical and subcortical point for subsequent group-level analyses.

Probabilistic distribution of cortical and subcortical functional responses

The MNI location x corresponds to an individual DES-induced functional response for a given function R (e.g. semantic, motor, etc.) in a single patient. The null hypothesis tested in our methodology was that no functional response was present at a given cortical or subcortical site (rather than a different functional response). As previously detailed,[22] based on the diameter of the bipolar DES electrode (5mm), we assume that all voxels y of the brain in MNI space at a distance ≤ 0.5 cm from x have the same functional response R. Also, similar to the aforementioned analysis,[13,21,22,24] let $R_1, \dots, R_k$ be the set of k functional responses considered in this study (e.g. semantic, motor, etc.), and let x be a voxel of the brain in the MNI space. We assume that any voxel x is associated with a vector $\boldsymbol{\pi}(x) = (\pi_1(x), \dots, \pi_k(x))$, where $\pi_i(x)$ is the probability that voxel x is involved in the processing of the functional response R_i. Let us assume that $n(x)$ functional response errors have been induced by DES at voxel x in our patient series, obtaining $l_i(x)$ functional response errors of type R_i, with $\sum_{i=1}^{k} l_i(x) = n(x)$. We assume that the number of outcomes $l_i(x)$ follows a multinomial distribution with parameters $n(x)$ and $\boldsymbol{\pi}(x)$. Therefore, the probability function of this multinomial distribution is:

$f(l_1(x), \dots, l_k(x); n(x), \pi(x)) = \frac{n(x)!}{l_1(x)! \cdots l_k(x)!} \pi_1^{l_1(x)}(x) \cdots \pi_k^{l_k(x)}(x)$. The maximum likelihood estimate of any individual probability $\pi_i(x)$is $p_i(x) = l_i(x)/n(x)$. Maximum likelihood estimates $p_i(x)$, derived by varying x in the MNI space, represent statistical maps in the MNI

space of the probability that voxels x are involved in the processing of functional responses R_i. As a check of validity of the proposed method, statistical maps $p_i(x)$ consistently match with those previously reported.[21,22]

Matching analysis

In order to provide a quantitative analysis of the data, for comparison with recent literature, and to validate our stimulation point localization technique, we performed a partition of our brain model into 176 cortical and cortical plus white matter anatomical ROIs, according to the extensively adopted JHU Atlas.[40] For each spatial map $p_i(x)$, we computed the percentage of the maps of the functional responses overlapping the ROIs of this anatomic atlas.

Finally, we computed the distance of any subcortical functional response from all the WM pathways of the tractography atlas of NatBrainLab (available at: http://www.natbrainlab.co.uk/atlas-maps)[41]. The distance of a stimulus from a given bundle of the atlas was defined as the minimal Euclidean distance between the stimulus and the set of voxels defining the tract itself, as previously described.[22] This allowed us to quantify the distribution of the distance of the different functional responses R_i from the main bundles of the human WM, as reconstructed in the most recent version of this established tool.

RESULTS

An overall number of 1821 positive responses were collected by using DES (1162 cortical, 659 subcortical) among 16 functional domains.

Cortical functional responses collected included: reading (2), anomia (94), asemantism [i.e. comprehension disorders during execution of PPTT (17)], eye movement control (4), mentalizing (12), motor (325), motor control (89), phonological (14), semantic (39), somatosensory (150), spatial perception (23), speech output (251), speech articulation (142). Subcortical functional responses included: acoustic (2), reading (13), anomia (31), non-verbal comprehension (20), eye movement control (7), language and motor planning (24), mentalizing (14), motor (103), motor control (72), phonological (69), semantic (131), somatosensory (69), spatial perception (12), speech output (27), speech articulation (42), and visual (23).

The probabilistic distribution of the cortical and subcortical responses for each function among the entire patient cohort is reported in Figures 2, 3 and 4. Sagittal, coronal, and axial slices (spacing = 10 mm) along the respective MNI coordinates (x, y, z), illustrate the probability distribution, including a color scale reflecting the confidence interval of each function, plotted onto the MNI 152 brain template and based on the multinomial statistical analysis.

For example, the first two panels of Figure 2 report the distribution of motor and sensory responses, with the highest probability voxels, as expected, in the mid-portion of the pre- and post-central gyri, respectively.

The results of the matching analysis of the DES-defined functional responses with the major subcortical pathways as reconstructed in NatBrainLab Atlas are shown in the graphs of Figure 5. Data are presented as the distance from subcortical DES points to the known WM pathways.

Finally, the overlap of DES-based data with the cortical and the cortical *plus* superficial WM ROIs of the JHU Atlas are reported in Tables 2 and 3.

DISCUSSION

General considerations

Brain disorders represent an increasingly important problem for public health, given the high incidence and costs of diagnosis/treatment, as well as the increased level of physical and social disability, as the worldwide population ages.[30] Accordingly, understanding the functional and structural organization of the human brain has been a key challenge not only for the neuroscience but also for the medical community. Recently, the National Institutes of Health in the United States established the Human Connectome Project (HCP), with the goal of mapping critical human brain structures and functions in healthy subjects over the lifespan. While the HCP has primarily focused on neuroimaging data in healthy subjects, multimodal research methods in both healthy and patient populations will be needed to develop reliable maps of human brain networks.[42]

We computed a detailed three-dimensional probability distribution atlas for critical human brain functions with the largest stimulation-based functional dataset of the human brain to date (1187 functional responses in 256 patients). This “heat map” has, as an unprecedented feature, the capacity to integrate direct functional responses at both the cortical and the subcortical level obtained by stimulation. As a consequence, it may serve as a minimal and highly-specific anatomic-functional background for integration with different neuroimaging data as well as other functional (fMRI, TMS, EEG, etc.) and structural (i.e. tractography) datasets, with the goal of resolving the “true” governing principles behind physiologic brain processing, as well as patterns of reorganization following injury, i.e. neuroplasticity.

Functional considerations

1. **Motor and somatosensory—**The distribution of involuntary movements at DES reflects the classical cortical-subcortical distribution of the primary motor system, involving the pre-central gyrus (PreCG) and the corticospinal (CS) pathway (Figure 2).[9,22,43] Sensory stimuli are distributed according to the classical cortical-subcortical organization of the somatosensory system, including the post-central gyrus (PostCG) and the thalamo-cortical pathways (Figure 2. However, considering together these motor and sensory responses, our results suggest a non-rigid separation between the PreCG and the PostCG, as initially described by Penfield.[43] Rather, a strict reciprocal integration between the motor and sensory networks emerges, subserved by short inter-gyral WM connections.[44] It is worth noting the high overlap of the cortical and subcortical responses with the Pre- and Post-CG ROIs of the JHU Atlas (Table 2) and the course of the tractography pathways (see also graphs in Figure 5) confirms the reliable alignment of the data in the MNI space.

2. **Motor control and language/motor planning—**The distribution of the stimuli related to disorders of motor initiation and control, including movement arrest, confirms that awareness and control of voluntary movements depend on a network involving the dorsal-medial and lateral pre-motor cortices as well as the basal ganglia (Figure 2). A complex framework of inhibitory and excitatory connections with a somatotopic organization characterizes this circuitry.[45] In particular, the cortical distribution of stimuli related to interruption of the motor task confirms the key role of supplementary motor area (SMA), PreSMA, dorso-lateral pre-motor cortex (DLPMC), PreCS, insula and basal ganglia in the so-called "negative motor network" necessary for movement selection and pacing of voluntary movements.[9,22,46-48] A complex network of short and mid-range cortico-cortical and cortico-striatal fibers connects these regions, running in the deep WM of the frontal lobe (anteriorly to the pyramidal tract responsible for pure motor responses).[44,47] Language and motor planning errors resulting in motor/verbal perseverations (Figure 2 occurred predominantly during subcortical stimulation and mainly at the level of the caudate or neighboring WM. These results confirm the crucial role of the caudate in integrating the cortico-basal ganglia circuitry for the initiation, execution and control of movements.[49]

3. **Eye movement control—**Disorders of eye movements have a cortical-subcortical distribution at the posterior part of the middle frontal gyrus (MFG) in both hemispheres (Figure 2), which corresponds to the frontal eye fields. These results confirm the participation of this region in the network mediating motor initiation and control[9] with a concordant topography with respect to the definition of the crucial region for control of eyes movement and integration in spatial working memory.[50]

4. **Speech output—**The representation of cortical and subcortical speech output response errors (speech arrest) is bilateral and symmetrical, confirming a prevalent distribution within the most ventral portion of the pre-motor cortex and the underlying WM (Figure 3).[21,22] The occurrence of complete speech arrest after stimulation of the ventral pre-motor cortex (VPMC), as previously reported by regardless of the side stimulated, suggests a possible bi-hemispheric integration of the articulatory loop network as previously proposed in detailed stimulation study[21] and recently highlighted in multimodal study integrating resting-state fMRI and DES.[51]

5. **Speech articulation—**The cortical and subcortical distribution of speech articulation errors (verbal apraxia) during stimulation in the ventral cortices of the PreCG, PostCG, supramarginal gyrus (SMG), and in the underlying WM (Figure 3), including the indirect anterior component of superior longitudinal fascicle (SLF),[52] confirms the crucial role of the VPMC and this fronto-parietal network for converting the phonological information in articulatory motor output.[53] This characterization of speech articulatory network is concordant also with analysis combining resting-state fMRI, DES and tractography[51] and with CCEPs studies in humans.[14,54]

6. **Anomia—**The high frequency of subcortical anomia at the junction below the posterior temporal cortices [middle and posterior thirds of STG and middle temporal gyrus (MTG)] and the inferior parietal lobule [particularly, the angular gyrus (AG)](Figure 3), matching the

course of the indirect posterior component of SLF, is likely a consequence of deactivation of visuo-semantic integration.[55] In fact, the temporal-parietal-occipital junction represents a crucial region for visual-semantic processing and integration of this functional substrate into the dorsal stream.[56,57] From an anatomical point of view, this region includes an intersection of terminations of dorsal and ventral pathways [namely, indirect anterior and posterior SLF, arcuate fascicle (AF), inferior longitudinal fascicle (ILF), inferior fronto-occipital fascicle (IFOF)], as seen in the dorso-ventral posterior frontal lobe [namely, inferior frontal gyrus (IFG) and DLPFC] where terminations of IFOF, indirect anterior SLF and uncinated fascicle (UF) are adjacent and may overlap.[24,55,57]

7. Semantic—As indicated by the cortical and subcortical distribution of semantic paraphasias (Figure 3), semantic processing is supported by a large and distributed network, including the posterior and middle thirds of the STG and MTG, respectively, the DLPFC, and the IFG.[58] The subcortical distribution of semantic responses reflects the continuous and homogenous ventral course of functional information in the deep WM of the temporal lobe, from the occipital-temporal-parietal junction, through the ventral third of the external capsule, and ascending to the WM underneath the posterior two-thirds of IFG and MFG. This ventral workflow is crucial for the top-down control and contextualization of the semantic system.[9,59] It is mainly subserved by IFOF, as confirmed in this series by the consistent overlap of subcortical and cortical semantic responses with the course of the IFOF (Figure 5), from the posterior WM of the temporal lobe through the external capsule and up to its main territories of terminations within the frontal lobe (ventro-lateral and dorso-lateral cortices).[22,24,60,61] The IFOF is the longest association bundle in the human brain, with the unique feature of terminating in the occipital, temporal, parietal, and frontal lobes.[60-63] This long-range link between distant functional nodes was demonstrated to be crucial in mapping visual information into meaning, according to the classical role of the ventral stream.[9,22,28,64]

8. Non-verbal comprehension disorders—Non-verbal comprehension disorders identified with palm-pyramid-tree test (PPTT) were mainly located in the right hemisphere with a cortical distribution analogous to semantic paraphasias in the left hemisphere (Figure 3). In fact, these responses are distributed across the parietal, temporal and frontal regions with a prevalent ventral course matching with the course of the IFOF, in particular at the level of the WM of the ventral third of the external capsule between the temporal and frontal lobes. These data support the hypothesis of a hemispheric segregation between verbal and non-verbal semantics,[33,59] with the latter mediated by the right IFOF.[65]

9. Phonologic—Phonological disturbances revealed a large and typical distribution over the cortices and subcortical WM connecting the ventral and mid-dorsal cortices of the posterior frontal lobe (particularly, IFG and MFG) with the posterior two-thirds of the temporal lobe (particularly, STG and MTG)(Figure 3). We found a consistent match of the cortical and subcortical responses with the course and terminations of the AF. This multi-layer bundle[24,66] is the main component of the dorsal pathways and constitutes the essential structural core for long-range connection among the phonological epicenters that are largely distributed around the peri-sylvian cortices.[41,53,67,68] The parallel course of the two main

components of dorsal stream, AF (medially) and indirect anterior SLF (also known as SLF III, laterally) that connects the ventral frontal lobe with the inferior parietal lobule (IPL), [24,52,55] reflects the parallel and segregated distribution of, respectively, subcortical phonological and verbal apraxia responses. The adjacent and partially overlapping territories of termination of these bundles in the frontal lobe and IPL also reflects the distribution of the phonological and verbal apraxia responses at the cortical level, as in previous reports.[24,69] This intricate functional anatomy constitutes the essential background for the strict integration of the dorsal route. Our data suggest that in this system, auditory and somato-sensory speech inputs are transferred via direct AF fibers from the posterior two thirds of STG/MTG to the IFG (particularly, pars opercularis and triangularis), to be converted in working phonological–phonetic representations. This information is then translated into articulatory motor outputs mediated by the VPMC, which receives feedback information from somatosensory and auditory areas at the junction between STG and SMG and the ventral PostCG, via the SLF III.[9,53]

10. Visual and reading—The distribution of visual deficits (Figure 4) reflects the classical distribution of visual pathways underlying the temporal-occipital regions, including the primary visual area and optic radiations.[37]

Reading deficits were mainly distributed in the left MTG and inferior temporal gyrus (ITG), and in the basolateral WM of ITG and fusiform gyrus (Figure 4), corresponding to the course of the dorsal portion of ILF.[24] These cortical territories are also known as the visual word form area (VWFA) and are structurally involved in the elaboration of visual information, integrating inputs coming from the ipsilateral and contralateral occipital pole, via the posterior-dorsal portion of ILF and CC, respectively.[56,70] The ILF is a double component long bundle connecting the dorso-lateral and ventral cortices of the occipital lobe to the antero-lateral and anterior and basal temporal cortices.[24,57,71,72] This pathway is the main WM tract implicated in both the direct and indirect transfer of information between the occipital visual territories and temporal limbic and memory areas. The ILF subserves several aspects of visual input processing, such as face recognition, reading, visual perception and memory.[72] Finally, this occipital-temporal system is bi-directionally modulated by connections with the IPL, via the indirect posterior portion of SLF, connecting the posterior third of STG and MTG with the AG and the SMG, and providing an interactive feedback between visual and non-visual information.[56,73]

11. Spatial perception—Spatial perception error responses are strongly right-lateralized, as previously reported[74,75] and are distributed over the cortices of SMG, posterior portion of STG and within the WM crossing the IPL and the superior-posterior portion of the temporal lobe (Figure 4). This largely integrated cortico-subcortical network subserves the symmetrical processing of visual scene, attention and awareness. For this reason, several different qualitative and quantitative clinical manifestations have been described, depending on different patterns of cortical damage and WM disconnection. [25,75-77] The distribution of cortical and subcortical responses in this atlas confirmed that SMG and the posterior-superior STG are the main cortical hubs. Accordingly, the WM underlying the IPL, especially at the level of SMG where dorsal and ventral components of

SLF (i.e. II and III, respectively) have parallel course and adjacent terminations,[41,78-80] is the essential anatomical substrate for spatial awareness.[22,25,74] Finally, the subcortical responses elicited in the mid-dorsal WM of the frontal lobe, along the anterior course of SLF, highlight the basic fronto-parietal functional integration subserved by these fibers.[25,81]

12. Mentalizing—Mentalizing is a socio-cognitive process that enables humans to understand, and consequently predict, mental and psychological states (intentions or emotions) and behaviors of others. Previous studies demonstrated that mentalizing abilities are subserved by neural subsystems, namely the mirror neural network and the mentalizing network coding, respectively, for low-level perceptive socio-cognitive processes and high-level reflective processing.[82,83] In a previous work, the application of specific intraoperative behavioral tasks during DES mapping allowed to differentiate two functional sub-systems, respectively at the posterior infero-lateral prefrontal regions (low-level perceptual) and at the dorso-mesial prefrontal territory (high-level inferential).[13] The whole distribution of functional epicenters for mentalizing in the same portion of IFG and SFG (Figure 4) and in the WM of the frontal lobe connecting these ventral and dorsal cortices, confirms a crucial role of mid-posterior frontal lobe in different aspects of emotional and social cognitive intelligence.[84]

13. Acoustic—Acoustic responses were classically located along the posterior third of the *planum temporalis* and the WM underneath, connecting the auditory cortex of the Heschl's gyrus with the medial geniculate nucleus of the thalamus (Figure 4). Although no tractography atlas reconstructing the acoustic radiations are available, the subcortical distribution of these functional responses matches the course of the acoustic radiations, as recently renewed by high-resolution tractography and micro-dissection.[85]

Limitations

Our dataset, although unique given the different aspects highlighted above, does have some limitations. First, we propose data coming from a pathological model which assumes limited plasticity despite tumor involvement. Although tumor-induced plasticity may occur, LGGs have been shown to represent a valid model for exploring normal brain functions, and in fact, DES has been consistently utilized to confirm previous hypotheses of human brain processing.[9] As discussed above, the overall distribution of the functional responses is topographically congruent with the atlases used for matching analyses and the current literature, including large meta-analysis involving healthy human subjects. Finally, the large number of responses in this study (1821 responses in 256 patients) of patients with widely distributed tumor locations should minimize the contribution of plasticity effects in individual patients to our overall statistically-derived functional maps.

A second limitation relates to the collection of only positive functional responses in our series, in spite of a homogenous distribution of these responses over the brain at both cortical and subcortical levels. To minimize this possible issue, we adopted a solid multinomial statistical analysis and provided the confidence intervals plots of the positive critical nodes across our large functional datasets for both number of stimulations and subjects tested. The exploration with DES of the entire exposed cortex and subcortical WM

in each mapping session, including beyond the margins of the tumor, contributed to provide reliability to this data set.

Third, we utilized a linear transformation methods for normalizing patients brains to the MNI-125 atlas. While this may introduce some degree of error during normalization, we found that the linear approach worked best in our dataset, due to a combination of factors including brain shift, local mass effect, resection cavity distortion, and ventricular changes. The consistent matching of our data with prior independently published cortical/subcortical atlases (which was a second check of reliability) confirms that our registration approach was reasonable and accurate.

Lastly, given time limitations of surgery we were unable to test all 16 functional domains at each cortical and subcortical point, which may have biased our mapping of some functions to certain anatomic locations.

CONCLUSIONS

We computed the first integrated cortical-subcortical multi-functional probabilistic map of human brain processing, as emerged from direct electrical mapping during clinical and neuropsychological testing. The data discussed are concordant with the current literature and different multi-modal studies, and also provide new insights into the structural and functional organization of different networks. Finally, the unprecedented volume of functional responses collected, the large number of patients included, and the unique value of the WM distribution of the functional responses reported, allow for a reliable and complementary tool for multi-modal analyses exploring the structure and function of brain processing in humans.

Acknowledgments

Funding: This work has no sponsors.

REFERENCES

1. Crivellato E & Ribatti D Soul, mind, brain: Greek philosophy and the birth of neuroscience. Brain Res. Bull 71, 327–336 (2007). [PubMed: 17208648]
2. Hutchison RM et al. Dynamic functional connectivity: Promise, issues, and interpretations. Neuroimage 80, 360–378 (2013). [PubMed: 23707587]
3. Sporns O The human connectome: Origins and challenges. Neuroimage 80, 53–61 (2013). [PubMed: 23528922]
4. Fox MD Mapping Symptoms to Brain Networks with the Human Connectome. N. Engl. J. Med 379, 2237–2245 (2018). [PubMed: 30575457]
5. Petersen SE & Sporns O Brain Networks and Cognitive Architectures. Neuron 88, 207–219 (2015). [PubMed: 26447582]
6. van den Heuvel MP et al. Proportional thresholding in resting-state fMRI functional connectivity networks and consequences for patient-control connectome studies: Issues and recommendations. Neuroimage 152, 437–449 (2017). [PubMed: 28167349]
7. Maier-Hein KH et al. The challenge of mapping the human connectome based on diffusion tractography. Nat. Commun 8, (2017).
8. Pujol S et al. The DTI Challenge: Toward Standardized Evaluation of Diffusion Tensor Imaging Tractography for Neurosurgery. J Neuroimaging 25, 875–882 (2015). [PubMed: 26259925]

9. Duffau H Stimulation mapping of white matter tracts to study brain functional connectivity. Nature Reviews Neurology 11, 255–265 (2015). [PubMed: 25848923]
10. Thiebaut de Schotten M et al. Direct evidence for a parietal-frontal pathway subserving spatial awareness in humans. Science 309, 2226–8 (2005). [PubMed: 16195465]
11. Rech F, Herbet G, Moritz-Gasser S & Duffau H Disruption of bimanual movement by unilateral subcortical electrostimulation. Hum Brain Mapp 35, 3439–3445 (2014). [PubMed: 24415356]
12. Sarubbo S et al. Structural and functional integration between dorsal and ventral language streams as revealed by blunt dissection and direct electrical stimulation. Hum. Brain Mapp 37, (2016).
13. Herbet G et al. Inferring a dual-stream model of mentalizing from associative white matter fibres disconnection. Brain 137, 944–959 (2014). [PubMed: 24519980]
14. Matsumoto R et al. Functional connectivity in the human language system: A cortico-cortical evoked potential study. Brain (2004). doi:10.1093/brain/awh246
15. Matsumoto R et al. Parieto-frontal network in humans studied by cortico-cortical evoked potential. Hum. Brain Mapp 33, 2856–2872 (2012). [PubMed: 21928311]
16. Michel CM & Murray MM Towards the utilization of EEG as a brain imaging tool. NeuroImage (2012). doi:10.1016/j.neuroimage.2011.12.039
17. Sanai N, Mirzadeh Z & Berger MS Functional Outcome after Language Mapping for Glioma Resection. N. Engl. J. Med 358, 18–27 (2008). [PubMed: 18172171]
18. Sanai N & Berger MS Intraoperative stimulation techniques for functional pathway preservation and glioma resection. Neurosurg. Focus 28, E1 (2010).
19. Duffau H et al. Contribution of intraoperative electrical stimulations in surgery of low grade gliomas: A comparative study between two series without (1985-96) and with (1996-2003) functional mapping in the same institution. J. Neurol. Neurosurg. Psychiatry 76, 845–851 (2005). [PubMed: 15897509]
20. Ius T, Angelini E, Thiebaut de Schotten M, Mandonnet E & Duffau H Evidence for potentials and limitations of brain plasticity using an atlas of functional resectability of WHO grade II gliomas: Towards a “minimal common brain”. Neuroimage 56, 992–1000 (2011). [PubMed: 21414413]
21. Tate MC, Herbet G, Moritz-Gasser S, Tate JE & Duffau H Probabilistic map of critical functional regions of the human cerebral cortex: Broca’s area revisited. Brain 137, 2773–2782 (2014). [PubMed: 24970097]
22. Sarubbo S et al. Towards a functional atlas of human white matter. Hum Brain Mapp 36, 3117–3136 (2015). [PubMed: 25959791]
23. Herbet G et al. Converging evidence for a cortico-subcortical network mediating lexical retrieval. Brain 139, 3007–3021 (2016). [PubMed: 27604309]
24. Sarubbo S et al. Structural and functional integration between dorsal and ventral language streams as revealed by blunt dissection and direct electrical stimulation. Hum Brain Mapp 37, 3858–3872 (2016). [PubMed: 27258125]
25. Thiebaut de Schotten M et al. Direct evidence for a parietal-frontal pathway subserving spatial awareness in humans. Science (80-.). 309, 2226–2228 (2005).
26. Hau J et al. Revisiting the human uncinate fasciculus, its subcomponents and asymmetries with stem-based tractography and microdissection validation. Brain Struct Funct 222, 1645–1662 (2017). [PubMed: 27581617]
27. Duffau H et al. New insights into the anatomo-functional connectivity of the semantic system: a study using cortico-subcortical electrostimulations. Brain 128, 797–810 (2005). [PubMed: 15705610]
28. Duffau H, Leroy M & Gatignol P Cortico-subcortical organization of language networks in the right hemisphere: An electrostimulation study in left-handers. Neuropsychologia 46, 3197–3209 (2008). [PubMed: 18708080]
29. Coello AF et al. Selection of intraoperative tasks for awake mapping based on relationships between tumor location and functional networks. J. Neurosurg (2013). doi:10.3171/2013.6.JNS122470
30. Mandonnet E, Sarubbo S & Duffau H Proposal of an optimized strategy for intraoperative testing of speech and language during awake mapping. Neurosurg. Rev 40, 29–35 (2017). [PubMed: 27194132]

31. Deloche G et al. The effects of age, educational background and sex on confrontation naming in normals; principles for testing naming ability. Aphasiology (1991). doi:10.1080/02687039108248566
32. Duffau H et al. Usefulness of intraoperative electrical subcortical mapping during surgery for low-grade gliomas located within eloquent brain regions: functional results in a consecutive series of 103 patients. J. Neurosurg 98, 764–78 (2003). [PubMed: 12691401]
33. Moritz-Gasser S, Herbet G & Duffau H Mapping the connectivity underlying multimodal (verbal and non-verbal) semantic processing: A brain electrostimulation study. Neuropsychologia 51, 1814–1822 (2013). [PubMed: 23778263]
34. Herbet G, Lafargue G, Moritz-Gasser S, Bonnetblanc F & Duffau H Interfering with the neural activity of mirror-related frontal areas impairs mentalistic inferences. Brain Struct. Funct (2015). doi:10.1007/s00429-014-0777-x
35. Montemurro N, Herbet G & Duffau H Right Cortical and Axonal Structures Eliciting Ocular Deviation During Electrical Stimulation Mapping in Awake Patients. Brain Topogr. (2016). doi:10.1007/s10548-016-0490-6
36. Gras-Combe G, Moritz-Gasser S, Herbet G & Duffau H Intraoperative subcortical electrical mapping of optic radiations in awake surgery for glioma involving visual pathways. J. Neurosurg 117, 466–473 (2012). [PubMed: 22794319]
37. Sarubbo S et al. The course and the anatomo-functional relationships of the optic radiation: a combined study with ‘post mortem’ dissections and ‘in vivo’ direct electrical mapping. J Anat 226, 47–59 (2015). [PubMed: 25402811]
38. Bartolomeo P, De Schotten MT & Duffau H Mapping of visuospatial functions during brain surgery: A new tool to prevent unilateral spatial neglect [5]. Neurosurgery (2007). doi: 10.1227/01.neu.0000306126.46657.79
39. Evans AC et al. Anatomical mapping of functional activation in stereotactic coordinate space. Neuroimage 1, 43–53 (1992). [PubMed: 9343556]
40. Zhang Y et al. Atlas-guided tract reconstruction for automated and comprehensive examination of the white matter anatomy. Neuroimage 52, 1289–1301 (2010). [PubMed: 20570617]
41. Thiebaut de Schotten M et al. Atlasing location, asymmetry and inter-subject variability of white matter tracts in the human brain with MR diffusion tractography. Neuroimage 54, 49–59 (2011). [PubMed: 20682348]
42. Toga AW, Thompson PM, Mori S, Amunts K & Zilles K Towards multimodal atlases of the human brain. Nature Reviews Neuroscience (2006). doi:10.1038/nrn2012
43. Penfield W & Boldrey E Somatic motor and sensory representation in the cerebral cortex of man as studied by electrical stimulation. Brain 60, 389–443 (1937).
44. Catani M et al. Short frontal lobe connections of the human brain. Cortex 48, 273–291 (2012). [PubMed: 22209688]
45. Rech F, Herbet G, Moritz-Gasser S & Duffau H Somatotopic organization of the white matter tracts underpinning motor control in humans: an electrical stimulation study. Brain Struct Funct 221, 3743–3753 (2016). [PubMed: 26459143]
46. Hoffstaedter F, Grefkes C, Zilles K & Eickhoff SB The ‘What’ and ‘When’ of Self-Initiated Movements. Cereb. Cortex (2012). doi:10.1093/cercor/bhr391
47. Schucht P, Moritz-Gasser S, Herbet G, Raabe A & Duffau H Subcortical electrostimulation to identify network subserving motor control. Hum. Brain Mapp 34, 3023–3030 (2013). [PubMed: 22711688]
48. Wolpe N et al. The medial frontal-prefrontal network for altered awareness and control of action in corticobasal syndrome. Brain (2014). doi:10.1093/brain/awt302
49. Alexander GE & Crutcher MD Functional architecture of basal ganglia circuits: Neural substrates of parallel processing. Trends Neurosci. 13, 266–271 (1990). [PubMed: 1695401]
50. Courtney SM, Petit L, Maisog JM, Ungerleider LG & Haxby JV An area specialized for spatial working memory in human frontal cortex. Science (80-.). 279, 1347–1351 (1998).
51. Zacà D et al. Whole-Brain Network Connectivity Underlying the Human Speech Articulation as Emerged Integrating Direct Electric Stimulation, Resting State fMRI and Tractography. Front. Hum. Neurosci (2018). doi:10.3389/fnhum.2018.00405

52. Catani M, Jones DK & Ffytche DH Perisylvian language networks of the human brain. Ann. Neurol 57, 8–16 (2005). [PubMed: 15597383]
53. Duffau H, Moritz-Gasser S & Mandonnet E A re-examination of neural basis of language processing: Proposal of a dynamic hodotopical model from data provided by brain stimulation mapping during picture naming. Brain Lang. 131, 1–10 (2014). [PubMed: 23866901]
54. Matsumoto R et al. Parieto-frontal network in humans studied by cortico-cortical evoked potential. Hum. Brain Mapp (2012). doi:10.1002/hbm.21407
55. Martino J et al. Analysis of the subcomponents and cortical terminations of the perisylvian superior longitudinal fasciculus: a fiber dissection and DTI tractography study. Brain Struct. Funct 218, 105–121 (2013). [PubMed: 22422148]
56. Zemmoura I, Herbet G, Moritz-Gasser S & Duffau H New insights into the neural network mediating reading processes provided by cortico-subcortical electrical mapping. Hum. Brain Mapp (2015). doi:10.1002/hbm.22766
57. De Benedictis A et al. Anatomo-functional study of the temporo-parieto-occipital region: Dissection, tractographic and brain mapping evidence from a neurosurgical perspective. J. Anat 225, (2014).
58. Whitney C, Kirk M, O'Sullivan J, Lambon Ralph MA & Jefferies E The neural organization of semantic control: TMS evidence for a distributed network in left inferior frontal and posterior middle temporal gyrus. Cereb. Cortex (2011). doi:10.1093/cercor/bhq180
59. Han Z et al. White matter structural connectivity underlying semantic processing: evidence from brain damaged patients. Brain 136, 2952–2965 (2013). [PubMed: 23975453]
60. Hau J et al. Cortical terminations of the inferior fronto-occipital and uncinate fasciculi: Stem-based anatomical virtual dissection . Front Neuroanat 10, 58 (2016). [PubMed: 27252628]
61. Caverzasi E, Papinutto N, Amirbekian B, Berger MS & Henry RG Q-ball of inferior fronto-occipital fasciculus and beyond. PLoS One 9, (2014).
62. Sarubbo S, De Benedictis A, Maldonado IL, Basso G & Duffau H Frontal terminations for the inferior fronto-occipital fascicle: Anatomical dissection, DTI study and functional considerations on a multi-component bundle. Brain Struct. Funct 218, (2013).
63. Martino J, Brogna C, Robles SG, Vergani F & Duffau H Anatomic dissection of the inferior fronto-occipital fasciculus revisited in the lights of brain stimulation data. Cortex 46, 691–699 (2010). [PubMed: 19775684]
64. Duffau H et al. New insights into the anatomo-functional connectivity of the semantic system: a study using cortico-subcortical electrostimulations. Brain 128, 797–810 (2005). [PubMed: 15705610]
65. Herbet G, Moritz-Gasser S & Duffau H Direct evidence for the contributive role of the right inferior fronto-occipital fasciculus in non-verbal semantic cognition. Brain Struct. Funct 222, 1597–1610 (2017). [PubMed: 27568379]
66. Fernandez-Miranda JC et al. Asymmetry, connectivity, and segmentation of the arcuate fascicle in the human brain. Brain Struct Funct 220, 1665–1680 (2015). [PubMed: 24633827]
67. Corina DP et al. Analysis of naming errors during cortical stimulation mapping: Implications for models of language representation. Brain Lang. (2010). doi:10.1016/j.bandl.2010.04.001
68. Maldonado IL et al. Surgery for gliomas involving the left inferior parietal lobule: new insights into the functional anatomy provided by stimulation mapping in awake patients. J. Neurosurg (2011). doi:10.3171/2011.5.JNS112
69. Vigneau M et al. Meta-analyzing left hemisphere language areas: Phonology, semantics, and sentence processing. NeuroImage 30, 1414–1432 (2006). [PubMed: 16413796]
70. Herbet G, Zemmoura I & Duffau H Functional Anatomy of the Inferior Longitudinal Fasciculus: From Historical Reports to Current Hypotheses. Front. Neuroanat (2018). doi:10.3389/fnana.2018.00077
71. Catani M, Jones DK, Donato R & Ffytche DH Occipito-temporal connections in the human brain. Brain 126, 2093–2107 (2003). [PubMed: 12821517]
72. Mandonnet E, Gatignol P & Duffau H Evidence for an occipito-temporal tract underlying visual recognition in picture naming. Clin. Neurol. Neurosurg 111, 601–605 (2009). [PubMed: 19414212]

73. Dehaene S, Cohen L, Sigman M & Vinckier F The neural code for written words: A proposal. Trends in Cognitive Sciences (2005). doi:10.1016/j.tics.2005.05.004
74. Thiebaut de Schotten M et al. A lateralized brain network for visuospatial attention. Nat Neurosci 14, 1245–1246 (2011). [PubMed: 21926985]
75. Thiebaut de Schotten M et al. Damage to White Matter Pathways in Subacute and Chronic Spatial Neglect: A Group Study and 2 Single-Case Studies with Complete Virtual 'In Vivo' Tractography Dissection. Cereb. Cortex (2012). doi:10.1093/cercor/bhs351
76. Doricchi F, Thiebaut de Schotten M, Tomaiuolo F & Bartolomeo P White matter (dis)connections and gray matter (dys)functions in visual neglect: Gaining insights into the brain networks of spatial awareness. Cortex 44, 983–995 (2008). [PubMed: 18603235]
77. Verdon V, Schwartz S, Lovblad K-O, Hauert C-A & Vuilleumier P Neuroanatomy of hemispatial neglect and its functional components: a study using voxel-based lesion-symptom mapping. Brain 133, 880–894 (2010). [PubMed: 20028714]
78. Makris N et al. Segmentation of Subcomponents within the Superior Longitudinal Fascicle in Humans: A Quantitative, In Vivo, DT-MRI Study. Cereb. Cortex 15, 854–869 (2005). [PubMed: 15590909]
79. Vallar G et al. Cerebral correlates of visuospatial neglect: A direct cerebral stimulation study. Hum. Brain Mapp (2013). doi:10.1002/hbm.22257
80. Wang X et al. Subcomponents and connectivity of the superior longitudinal fasciculus in the human brain. Brain Struct Funct 221, 2075–2092 (2016). [PubMed: 25782434]
81. Lunven M et al. White matter lesional predictors of chronic visual neglect: a longitudinal study. Brain 138, 746–760 (2015). [PubMed: 25609686]
82. Amodio DM & Frith CD Meeting of minds: the medial frontal cortex and social cognition. Nat Rev Neurosci (2006). doi:10.1038/nrn1884
83. Molnar-Szakacs I & Uddin LQ Self-Processing and the Default Mode Network: Interactions with the Mirror Neuron System. Front. Hum. Neurosci (2013). doi:10.3389/fnhum.2013.00571
84. Yordanova YN, Duffau H & Herbet G Neural pathways subserving face-based mentalizing. Brain Struct. Funct (2017). doi:10.1007/s00429-017-1388-0
85. Maffei C et al. Topography of the human acoustic radiation as revealed by ex vivo fibers micro-dissection and in vivo diffusion-based tractography. Brain Struct. Funct 223, (2018).

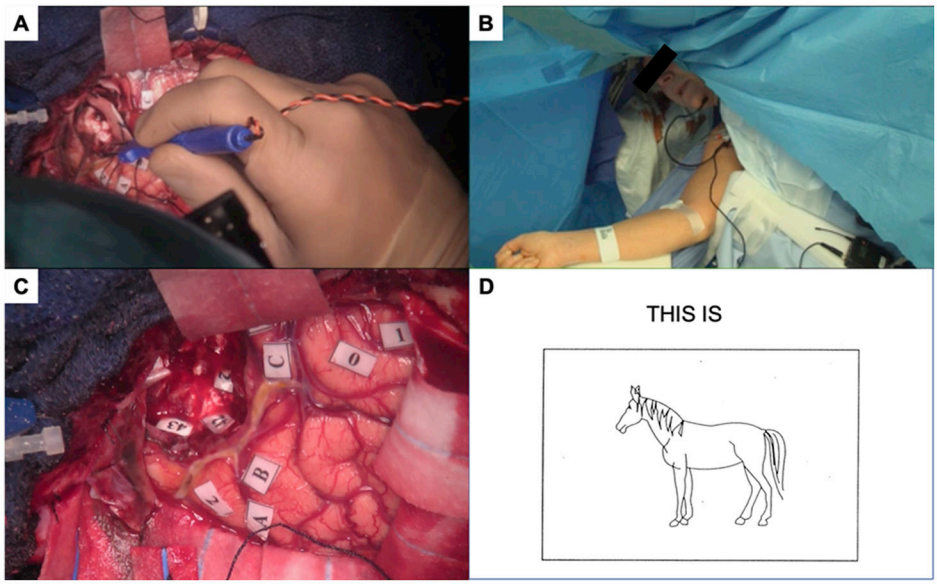

Figure 1. Intra-operative direct electrical stimulation-based mapping.

In panel A, the surgeon is stimulating the subcortical white matter of the middle temporal gyrus using a standard handheld bipolar stimulator while the patient (panel B) is performing a classical naming task. Panel C shows the final cortical (tags 0,1,2,A,B,C) and subcortical (42,43) positive mapping sites. For the naming task, the patient is asked to name the object presented on a computer screen (D) while the neurosurgeon stimulates sites at the cortical and subcortical white matter. In this case, the correct response is “This is a horse.” If the patient makes an error during stimulation at a particular site, the type of error is noted, such as anomia (patient says “This is a .....” but cannot come up with “horse”), semantic paraphasias (e.g. patient incorrectly says “This is a cow.” instead of “This is a horse.”), phonemic paraphasias (e.g. patient incorrectly says “This is a hearse.” instead of “This is a horse.”), speech arrest (no verbal output), or verbal perseveration (patient correctly says “This is a horse” but when a different object is shown after a delay, the patient incorrectly states “This is a horse.” again). In the example depicted in this figure, stimulation of the white matter region corresponding to site 42 (Panel C) caused an anomia. The MNI coordinates (x,y,z) corresponding to site 42 is derived by normalizing this patient’s brain to MNI space and manually plotting this subcortical point onto the normalized brain. For the group mapping and matching analyses, this point is combined with normalized coordinates of all other anomia sites from the entire cohort of subjects.

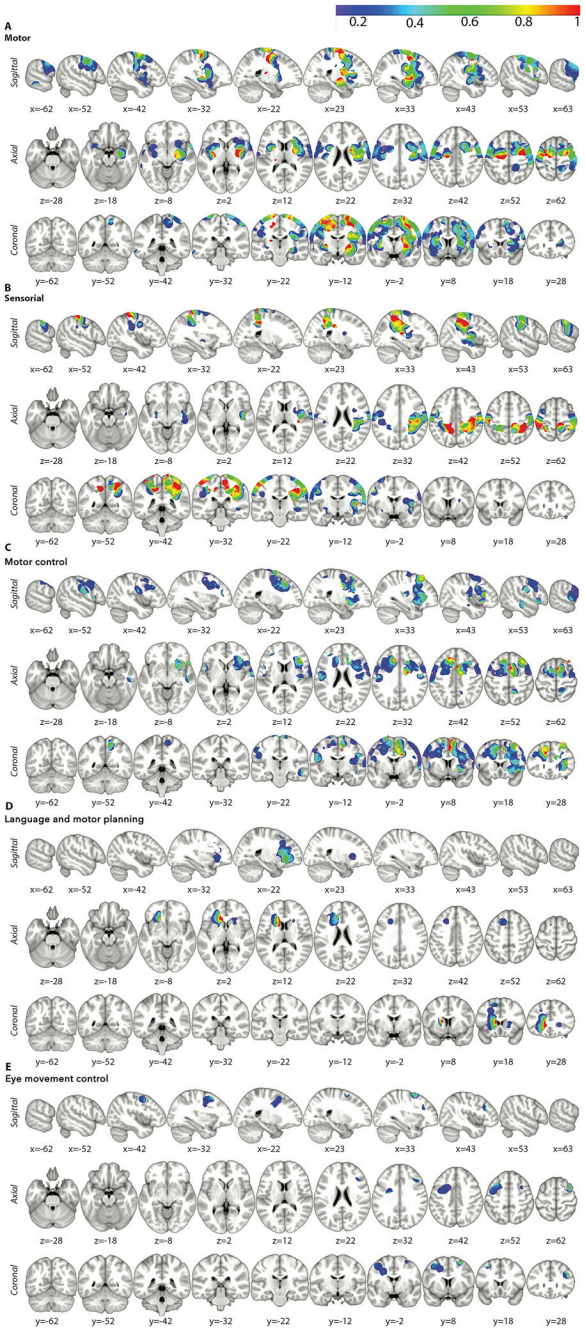

Figure 2.

The probability distribution along with confidence intervals mapped onto volumetric (1 mm) MNI T1 background (axial, sagittal, and coronal planes; 10 mm spacing) are demonstrated for the following functional responses: motor (A), somatosensory (B), motor control (C), language and motor planning (D), and eye movement control (E).

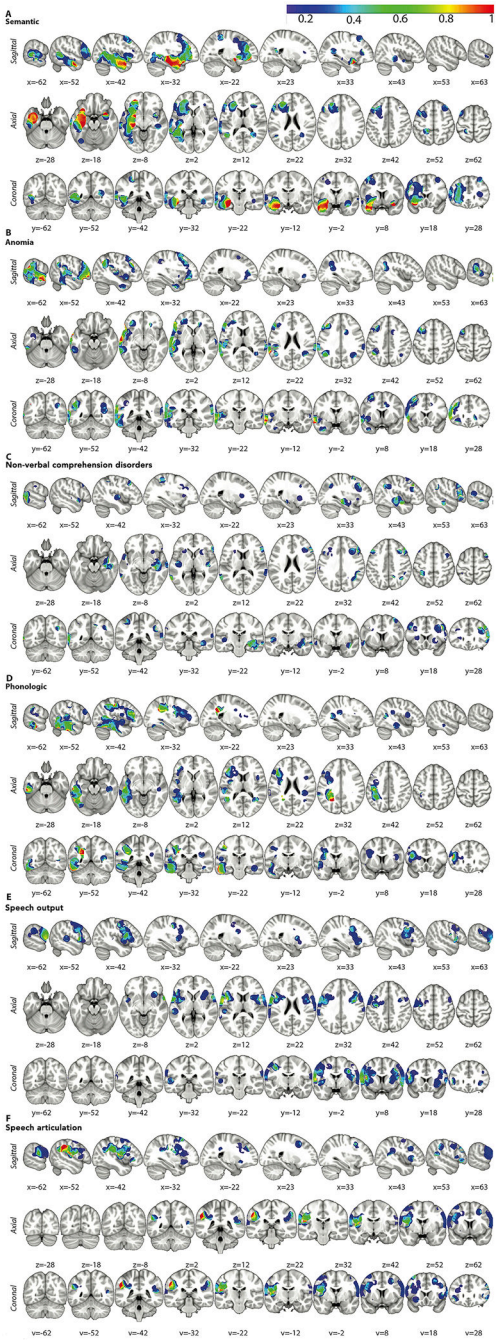

Figure 3.

The probability distribution, along with confidence intervals, mapped onto volumetric (1 mm) MNI T1 sequences (axial, sagittal and coronal planes; 10 mm spacing) are plotted for the following functional responses: speech output (A), speech articulation (B), anomia (C), semantic (D), non-verbal comprehension disorders (E), and phonologic (F).

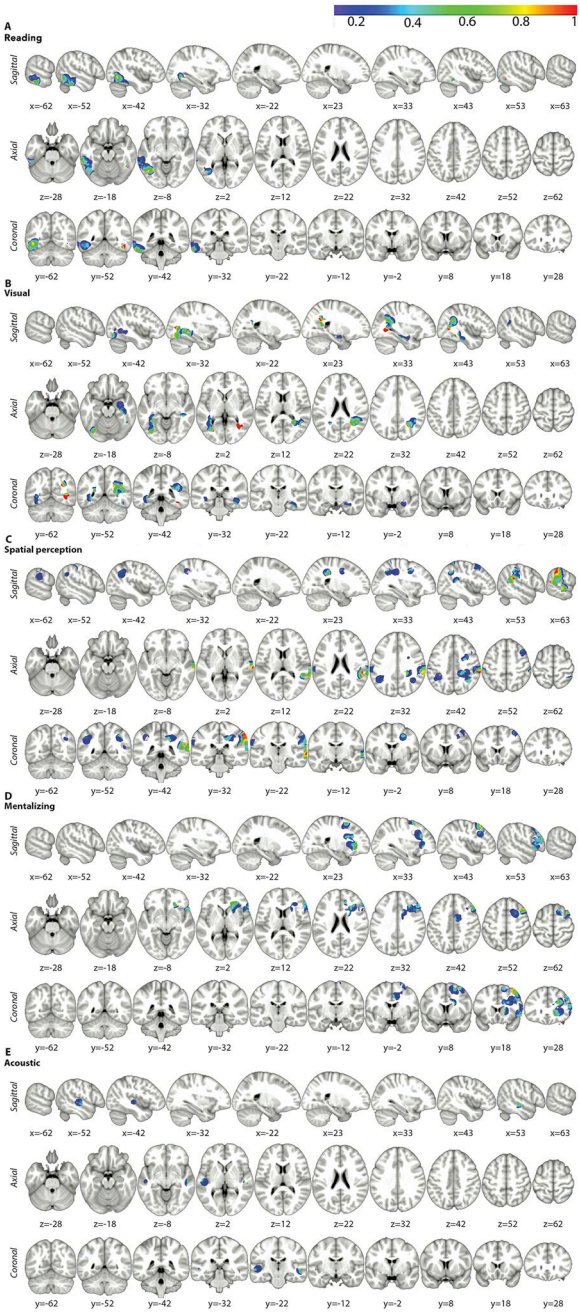

Figure 4.

The probability distribution, along with confidence intervals, mapped onto volumetric (1 mm) MNI T1 sequences (axial, sagittal and coronal planes; 10 mm spacing) are plotted for the following functional responses: visual (A), reading (B), spatial perception (C), mentalizing (D), and acoustic (E).

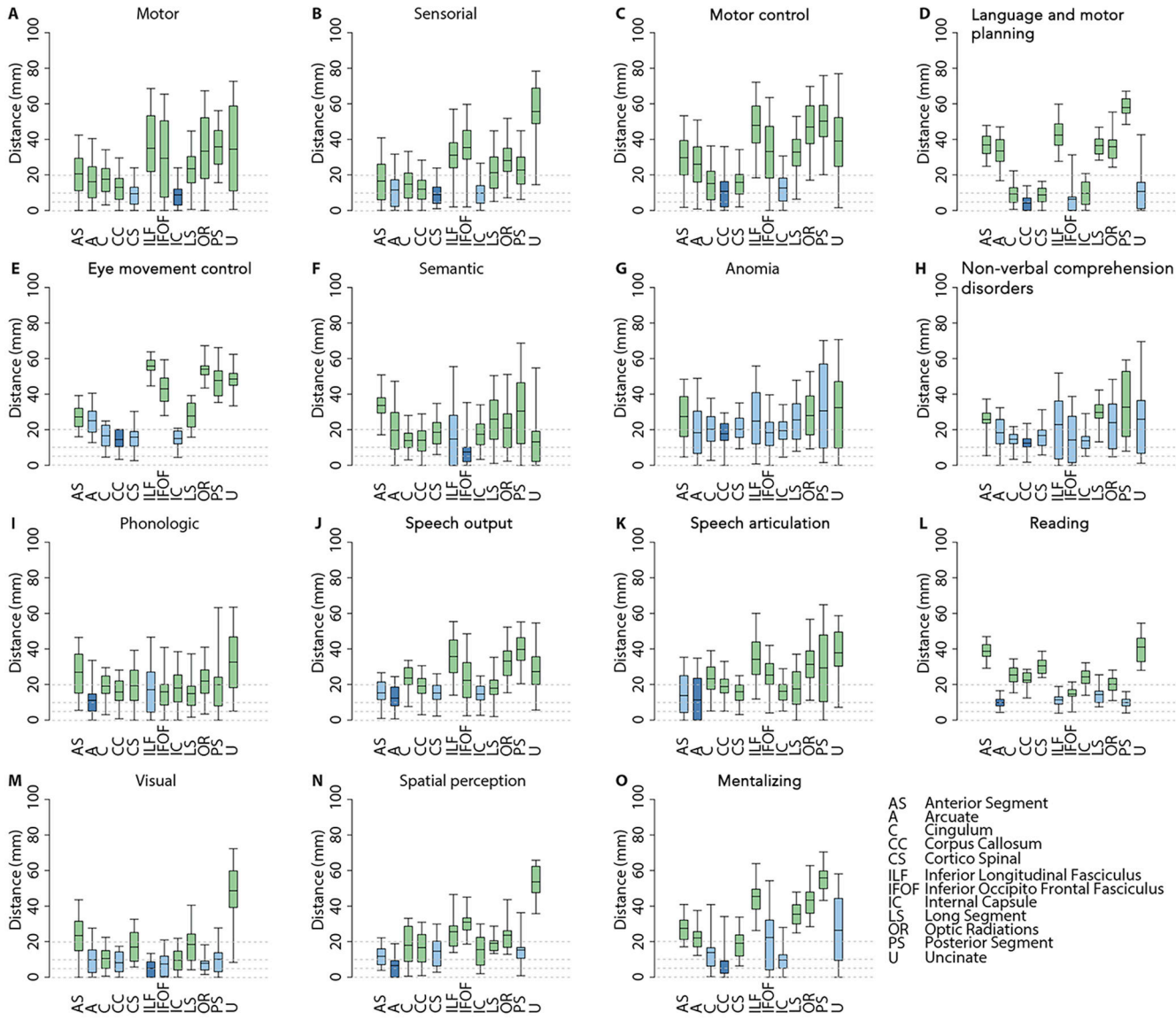

Figure 5.

In panels A-O we report the distributions (mean, 50% and 95% quantiles) of the distance of the different subcortical functional responses from the course of main white matter tracts, as reconstructed in the NatBrainLab Atlas (available at http://www.natbrainlab.co.uk/atlas-maps). In each panel the dark blue box plot represents the tract with minimal mean distance; the light blue box plots represent tracts whose mean distance is not statistically different from the minimal distance (Wilcoxon test; $p>0.05$); and the green box plots represent tracts whose mean distance is statistically different from the minimal distance (Wilcoxon test; $p<0.05$).

Table 1.

Patients demographics.

Patients (N°)	**256**
Age at surgery (years)	38.7 ±10.3
Male/Female	135/121
Tumor location (%)	
left	60.6
right	39.4
Handedness (%)	
right	85.1
left	9.4
ambidextrous	5.5
Tumor Distribution	**%**
Frontal	69
Temporal	56
Fronto-temporo-insular	40
Fronto-insular	32
Parietal	23
Temporo-insular	18
Temporo-parietal	8
Insular	2
Fronto-parietal	2
Temporo-occipital	2

Table 2.

Overall distribution of the functional responses elicited at the cortical level according to a matching analysis with the JHU Atlas (cortical and cortical *plus* white matter ROIs).

For each functional category, the percentage of DES-defined positive cortical sites that overlap with a given ROI is presented. For example, 32.4% of cortical sites where anomia was elicited with direct electrical stimulation overlapped with the JHU Atlas-defined left superior temporal gyrus, and 1.3% overlapped with the JHU Atlas-defined superior temporal gyrus white matter. MFG: middle frontal gyrus; MTG: middle temporal gyrus; IFG: inferior frontal gyrus; ITG: inferior temporal gyrus; PreCG: pre-central gyrus; PostCG: post-central gyrus; SFG: superior frontal gyrus; SMG: supra marginal gyrus; SPL: superior parietal lobule; STG: superior temporal gyrus; WM: white matter.

	Left hemisphere	Right hemisphere
Alexia	MTG (90.3%), ITG (7.2%), MTG WM (2.4%)	-
Anomia	STG (32.4%), ITG (17.1%), MTG (17.1%), MFG (10.2%), SMG (4.7%), IFG WM (2.3%), STG WM (1.3%)	STG (2.4%)
Comprehension	MTG (20.3%), MFG (8.9%), STG (7%),	MFG (24.9%), IFG (16.5%), STG (6.3%), MTG (5.3%), MFG WM (2.3%), IFG WM (1.6%), SMG (1.3%)
Eye Movement Control	-	PreCG WM (65.9%), PreCG (27.1%), PostCG (7.1%)
Mentalizing	-	MFG (62.1%), IFG (22%), SFG (6.6%), MFG WM (6.5%), IFG WM (2.7%)
Motor	PreCG (18.2%), PostCG (8.3%), MFG (6.7%), PreCG WM (2.5%), SFG (1.9%), IFG (1.1%)	PreCG (22.7%), PostCG (12.3%), SFG (5.2%), MFG (4.9%), PreCG WM (4.1%), IFG (2.1%), STG (1.8%), PostCG WM (1.7%), SPL (1.2%)
Motor Control	MFG (9.9%), SFG (8.8%), PreCG (7%), PostCG (4.4%), SMG (2.3%), PostCG WM (1.7%), PreCG WM (1.5%), IFG (1%)	PreCG (26.4%), MFG (9.1%), STG (8.3%), SFG (4.1%), PreCG WM (4%), IFG (4%), PostCG (2.7%), STG WM (1.1%)
Phonological	SMG (31.4%), MFG (22.9%), MTG (21.4%), IFG (12.6%), SMG WM (3.6%), MFG WM (2.7%), STG (2%), ITG (1.5%)	-
Semantic	MFG (24.2%), STG (22.5%), IFG (21.6%), MTG (20.1%), IFG WM (3.2%), MFG WM (2.6%), STG WM (1.5%), PostCG (1%)	STG (1.5%)
Somatosensory	PostCG (26%), PreCG (5.3%), PostCG WM (4.6%), SMG (3.4%), SPL (1.4%)	PostCG (32%), PreCG (6.1%), SPL (5.6%), PostCG WM (5.4%), SMG (5.4%)
Spatial perception	SMG (5.9%)	SMG (40.9%), STG (25.1%), MTG (8.7%), SMG WM (5.9%), MFG (4.1%), STG WM (3.2%), SPL (1.8%), MFG WM (1.5%)
Speech Output	PreCG (27.3%), IFG (11.1%), PostCG (10.6%), PreCG WM (4.3%), SMG (4%), STG (4%), MTG (3.9%), IFG WM (1.8%)	PreCG (10.4%), IFG (5.2%), STG (5%), PostCG (3.1%), PreCG WM (2%), SMG (1.8%), MFG (1.8%), IFG WM (1%)
Speech Articulation	PostCG (19.9%), MFG (9.1%), PreCG (7.4%), IFG (7.2%), SMG (4.5%), STG (3.7%), PostCG WM (1.5%), IFG WM (1.3%)	PreCG (14.8%), IFG (11.2%), MFG (5.4%), PostCG (5.4%), PreCG WM (3.4%), STG (1.7%)

Table 3.

Distribution of the functional responses elicited in the white matter according to the matching analysis with the ROIs of JHU Atlas (cortical and cortical *plus* white matter ROIs).

For each functional category, the percentage of DES-defined subcortical white matter positive sites that overlap with a given ROI is presented. For example, 28.4% of sites where alexia was elicited with direct electrical stimulation of the subcortical white matter overlapped with the JHU Atlas-defined inferior temporal gyrus, and 5.8% overlapped with the JHU Atlas-defined inferior temporal gyrus white matter. AG: angular gyrus; CG: cingulate gyrus; FG: fusiform gyrus; FOC: fronts-orbital cortex; MFG: middle frontal gyrus; MOG: middle occipital gyrus; MTG: middle temporal gyrus; IFG: inferior frontal gyrus; IOG: inferior occipital gyrus; ITG: inferior temporal gyrus; PreCG: pre-central gyrus; PostCG: post-central gyrus; SFG: superior frontal gyrus; SMG: supra marginal gyrus; SOG: superior occipital gyrus; SPL: superior parietal lobule; STG: superior temporal gyrus; WM: white matter.

	Left hemisphere	Right hemisphere
Acoustic responses	STG (31%), STG WM (21.1%), MTG (2.9%)	STG (20.4%), MTG (14.1%), STG WM (5.5%), MTG WM (4.9%)
Reading	ITG (28.4%), FG (21.5%), MTG (8.2%), IOG (6.5%), ITG WM (5.8%), MTG WM (5.3%), FG WM (5.2%), IOG WM (3.4%)	ITG (4.3%), ITG WM (2.4%)
Anomia	STG (11.5%), MFG (8.1%), MFG WM (7.8%), AG (7.4%), AG WM (7%), MTG (6.9%), ITG (6.6%)STG WM (4.1%), IFG WM (3.3%), SMG (2.9%), insula (2.6%), lateral FOC (2.5%), ITG WM (2.3%), MTG WM (2%), IFG (1.9%), SMG WM (1.3%), lateral FOC WM (1.1%), FG (1%)	AG WM (3.8%), AG (1.8%), MTG WM (1%)
Comprehension	SPL (3.3%), STG (3.2%), insula (2.9%), SPL WM (2.6%), SMG WM (2.1%), MFG WM (1.7%), STG WM (1.2%)	MFG WM (9.7%), STG (7%), hippocampus (6.9%), MFG (6.7%), STG WM (6.6%), AG WM (6.6%), MTG WM (4.9%), AG (3.9%), insula (3.6%), ITG WM (2.7%), ITG (2%), PostCG (1.2%), SMFG (1.2%), MTG (1.1%)
Eye movement Control	MFG (23.4%), MFG WM (19.3%), SFG WM (4%), PreCG (3.8%), PreCG WM (3.6%), SFG (2.2%)	MFG (19.6%), MFG WM (9.5%), SFG (3.8%), SFG WM (1.3%)
Language and Motor Planning	CN (13.9%), SFG WM (6%), SFG (4.9%), MFG WM (3%), insula (2.9%), IFG (2.4%), lateral FOC WM (2.1%), IFG WM (1.9%), MFG (1.8%), Putamen (1.4%), lateral FOC (1.1%)	CN (1.3%)
Mentalizing	-	MFG WM (12.4%), IFG (9.9%), MFG (9.2%), SFG (8.8%), IFG WM (6.7%), SFG WM (6.5%), CG (3.7%), CN (3.3%), insula (1%)
Motor	PreCG WM (5.2%), SFG (4.6%), PreCG (4.5%), SFG WM (4.2%), putamen (2.4%), insula (2.3%), MFG (1.7%)	preCG WM (5.9%), SFG (5.2%), putamen (4.9%), SFG WM (4.6%), PreCG (4.3%), insula (4.2%), MFG (3.3%), MFG WM (2.4%), PostCG (2.1%), SLF (2.1%), PostCG WM (1.6%), IFG (1.2%), IFG WM (1%)
Motor Control	SFG WM (8.9%), SFG (7.5%), MFG WM (3.4%), MFG (3.1%), CG (1.7%), PostCG WM (1.4%), PostCG (1.3%), preCG (1.1%)	SFG (10.3%), SFG WM (6.9%), MFG (4.9%), CG (4.7%), IFG (4.6%), IFG WM (4.2%), insula (2.8%), MFG WM (2.5%), putamen (1.9%), precuneus (1.4%)
Phonological	ITG (10.3%), MTG (8.4%), MTG WM (7.9%), FG (6.3%), IFG WM (5.8%), STG (4.9%), SPL WM (3.6%), ITG WM (3.2%), IFG (2.9%), MFG (2.8%), STG WM (2.7%), AG WM (2.4%), MFG WM (2.4%), PostCG WM (2%), SS (2%), PreCG WM (1.9%), AG (1.9%), PostCG (1.9%), SPL (1.8%), SMG WM (1.5%), PreCG (1.5%), SMG (1.4%), insula (1.2%)	-
Semantic	MTG WM (7.7%), insula (6.9%), MTG (5.7%), STG (5.5%), hippocampus (4.9%), MFG WM (4.6%), ITG (4.6%), ITG (4.6%), FG (4.4%), ITG WM (4.6%), STG WM (3.9%), MFG	-

	Left hemisphere	Right hemisphere
	3.2%), IFG (3.1%), IFG WM (2.7%), putamen (2%), lateral FOC (2%), FG WM (1.7%), SFG WM (1.3%)	
Somatosensory	SPL WM (6.2%), SPL (2.9%), PostCG WM (2.7%), precuneus (2.5%), PostCG (1.2%), preCG (1.2%), PreCG WM (1.1%)	SPL (8.6%), PostCG WM (8.3%), PostCG (8.1%), SPL WM (7.1%), SMG (6.7%), AG (4.6%), SMG (4.6%), insula (3%), pre-cuneus (2.4%), STG (2.2%), AG WM (2%), PreCG (1.7%)
Spatial perception	AG WM (6.7%), AG (6.2%)	SMG (17.1%), SMG WM (11.9%), AG (10.5%), AG WM (6.7%), STG (4.4%), SPL WM (4.2%), STG WM (3.3%), MFG WM (3.2%), PostCG WM (2.6%), SPL (1.9%), CG (1.6%), MTG (1.5%), PreCG WM (1.3%), MFG (1.3%)
Speech Output	IFG (11.4%), IFG WM (10.7%), PreCG (8%), PreCG WM (7.7%), MFG (5.2%), STG (5.1%), insula (4.1%), MFG WM (2.5%), STG WM (1.7%)	PreCG WM (6.1%), PReCG (6%), MFG (4.1%), IFG (3.8%), insula (3.6%), MFG WM (3.3%), IFG WM (3.1%), putamen (1.6%)
Speech Articulation	SMG WM (10.6%), SMG (10.5%), PostCG (6.1%), PreCG WM (6.1%), PostCG WM (5.2%), PreCG (5.1%), IFG (4.1%), MFG (4%), IFG WM (3.6%), MFG WM (3.2%), STG (3.1%), AG WM (2.9%), AG (2.8%), insula (2.5%), SFG WM (1.2%)	SMG (2.6%), SMG WM (2.4%), IFG (2.3%), MFG (2.2%), SFG WM (1.6%), MFG WM (1.3%)
Visual	FG (8.6%), IOG WM (3.1%), FG WM (2.9%), MOG WM (1.9%), IOG (1.5%)	AG WM (9%), AG (5.4%), IOG (4.1%), MTG WM (3.8%), MOG WM (3.3%), Hippocampus (3.1%), FG (2.7%), IOG WM (2.3%), SPL WM (2%), SOG WM (1.8%), MOG (1.6%), MTG (1.5%), ITG (1.5%), FG WM (1.2%), STG WM (1%), SMG WM (1%)